Evaluation of NDT techniques for the detection of kissing bond defects in composite joints

1. Abstract

Bonded joints are being increasingly used in various industries such as Aerospace, Defence, and Automobile industries etc. More and more aircraftstructural elements are manufactured out of composite materials thanks to the excellent rigidity to weight ratio. Bonded joints are extensively used to join aircraft parts because they offer compactness and defect free joints compared to the other joint types. In these joints, any small defect in the bonded area can lead to a catastrophic failure. There are many types of defects in bonded joints of composite parts such as porosity, internal voids, and no-bond regions etc. Researchers have devised various methods to detect the defects except one and that is kissing bond defects. Kissing bond defects are well known and are undetectable using any classical NDT method. As they are practically a zero-volume dis-bond defect, the joint is intact but with zero shear strength, leave no signature for usual NDT methods that identify discontinuities (cracks, porosities and gaps). The only way to reliably detect a kissing bond is by destructive mechanical testing showing the limited shear resistance. For the safe use of bonded joints in aerospace or defence industries, it is critical to developing an NDT technology for reliably detecting kissing bonds. In this regard, we have developed a protocol to fabricate bonded joints with kissing bonds. The created bonded joints with kissing bonds have been subjected to mechanical testing to confirm the creation of kissing bond defects. Extensive research has been carried out on developing advanced NDT techniques to detect the kissing bonds. Some of the techniques we have explored and tested are Ultrasonic Guided Waves, Laser Shock, High frequency C-scan and Computed Tomography.

Keywords: Kissing bond, Laser shock, guided waves, zero volume defects.

2. Introduction

Fabrication of defect free bonded joints is one of the challenges faced by various industries. This is due to the occurrence of practically undetectable defects such as kissing bond defect. It is well known that kissing bond defects are zero volume dis-bonds [1]. By definition, these bonds are undetectable using any of the classical non-destructive techniques (NDT) [2]. The only testing technique by which these defects can be detected is destructive testing [3]. The method destroys components hence it is not preferred.

An alternate method by which the defects can be detected is by employing advanced NDT methods.Testing with advanced ultrasound techniques or using a technique that is a combination of two or more NDT technologies tuned together has shown some favorable results [3 4].

Guided waves are used extensively in the field of structural health monitoring. These are the efficient waves for testing large scale structures because they enable line-to-line inspection capability. Using the property of guided waves, these are used for testing and defect detection in plates [567], railways [8], pipes [9].

Characteristics of guided wave propagation in anisotropic materials such as composites are presented by [10]. Steering the direction of the group velocity of the guided wave when there is complex material structure, the effect of damping, material structure on attenuation of waves are presented in the work.

The technique is used in the case of defect detection in bonded joints. Theoretical and experimental evaluation of lamb/guided waves interaction with bonded joints is studied by [11]. In the work, it is hypothesised and experimentally proved that the guided waves interact with a bonded joint. So, the transmitted waves through the bonded joint contain the information of the bond strength.Bond strength of

joints is investigated using a quasi-static model of interaction of ultrasonic-guided waves with imperfect joints/interfaces by[12]. In this work, the researcher has presented the details of how guided waves interact with bonded joints of varying strength. A correlation is made between the transmitted waves and the bond quality.A comparative study is presented by [13] on the interaction of guided waves with a healthy joint and a joint with defects. The bonded joint with kissing bond defect is created in various ways namely (i) Porous PTFE film insert (ii) Peel ply separation film (iii) Adhesive is removed before bonding (iv) Non-porous PTFE film insert (v) Adhesive layer removed (vi) Grease insertion. Air coupled C-scan and laser-vibrometer measurements are used to obtain the results. In [14] it is hypothesised that the transmission of guided waves is subjected to the existence of disbonding in the bonded joint. The existence of disbands results in transmitting some part of the lamb waves which are identified by producing a C-scan. Mode conversion of guided waves in composite bonded joints is investigated by [15]. It is based on the fact that there exist certain modes of guided waves which are sensitive to the defects in the composite material bonded joints. In addition there are several other works in the literature that present study and testing results of composite material, bonded joints for defect detection [16 17 18].

One of the setbacks of guided wave NDT is that there is a limitation on the frequency of operation. Setting up of guided waves is not possible at a high frequency of operation. Hence, an advantage of inspecting for small size defects is lost. However, high frequency operation is possible in A, B, C-scans. High frequency based NDT techniques are also used for effective defect detection in materials, joints[19]. Testing of composite material for defects is studied using a terahertz imaging technology by [20]. Single crystal based piezoelectric composites are developed by [21] for high frequency scan tests of composite material and composite bonded joints. The high-frequency high-resolution acoustic microscopy technique is used in [22] to detect weak bonds in bonded joints of composites.

Laser shock also known as laser peening is extensively used in the material processing industry to obtain required properties in the material [23]. The technique is one of the destructive techniques because it alters the materials internal and external structure. However, if the laser energy and pulse duration are optimized [24 25] to a particular material, the laser shock only creates shock waves within the material resulting in a non-destructive test.

In the literature, the technique used to estimate tensile strength of planar surfaces [2627] using laser shock.Using the strength estimation technique, Laser ultrasonic and laser-tapping technique is proposed by [24] for detachment, defect detection in material using short pulses. The defects include delamination in skin and detachment in between the skin and core in composites. The work also provides the information of utilizing the impact created by laser-tapping for non-destructive testing by tuning the pulse duration. In the study of [25] laser pulse induced spallation technique is used to determine the strength between coating and substrate. It also uses a similar principle of optimizing the laser energy and pulse duration for bond quality testing. Such techniques are also used by various researchers [28293031].

Laser ultrasonic testing is proposed by [32] which is a closed loop of a pulsed laser and a laser-vibrometer configured in a pulse-echo mode. This basic setup successfully detects delamination in the composite material. The setup is upgraded to laser tapping mode with which disbands are detected. A step-by-step laser power increase in the laser shock test is proposed by [33] in order to obtain the bond strength/quality of carbon-epoxy composite bonded joints. As the laser energy is increased step-by-step, it is possible to avoid destructive testing of the material. A similar method is proposed by [34]. In this work, the researchers give a scientific approach to optimize the laser energy and pulse for non-destructive tests. It also provides the study of damage created in composite test samples at different laser energies.Bond strength of composite material and bonded joint strength and disband detecting is done by [35]. Laser shock is used to obtain the results. The work presents a systematic way to evaluate composite material for its local strength, degradation of the material bonds over a long time.The composite bond quality evaluation is done by [36]

using laser shock. A special technique known as dip-coating is proposed to create kissing bond like defects. The test results of the bond with defect and without defect are compared to detect the weak adhesion bond in the joint. The discussed literature until now uses one pulsed laser to evaluate material, bonded joint. A novel laser configuration called symmetrical laser shock setup is proposed by [37 38] for composite material testing, defects such as delamination, disband creation and defect detection in the bonded joints.

In the methods discussed above, there is a significant setback with respect to 3D scanning of the material. This can be fulfilled using computed tomography (CT) scanning. This technique is capable of creating full a 3D reconstruction of samples. Hence, it is ideal for the identification of small defects. In the literature,X-ray computed tomography (CT) inspection of composites is presented in [39]. Non-destructive evaluation of complex composites is carried out by [40] using CT scan. One of the setbacks of CT-scan is the attenuation in complex materials such as composite. To overcome this, a dual energy computed tomography is used [41 42].

The aim of the present work is to create bonded joints with kissing bond defects and detect the same. For this purpose, several bonded joints are created. The existence of kissing bond defects in the bonded joints is confirmed by mechanical testing. Upon validating with mechanical testing, a standard protocol to create bonded joints with kissing bonds is established. Another set of bonded joints are created for NDT.
In the following sections, a detailed method of creating bonded joints with kissing bond defects is explained in Section 3. In Section 4, details of various advanced NDT methods used to detect kissing bond defects in the bonded joints are given. Experimental results of each NDT method are presented. Individual and comparative analysis of the results is done. The work is concluded in Section 5.

3. Kissing Bond manufacturing procedure

3.1 Details of material (Composite) used to fabricate the samples (GMI Aero)

In this study the test samples were fabricated using aeronautical grade materials provided by Dassault Aviation. All composite plates are consisted of twenty (20) plies of the HexPly M21/IMAprepreg, which is a toughened epoxy resin system supplied with unidirectional carbon fibers. The curing procedure was performed in an autoclave according to the specifications stated in the data sheet. The stacking sequence is illustrated in figure 1.

1	M21EV/IMA	0°	
2	M21EV/IMA	+45°	
3	M21EV/IMA	0°	
4	M21EV/IMA	-45°	
5	M21EV/IMA	0°	
6	M21EV/IMA	90°	
7	M21EV/IMA	0°	
8	M21EV/IMA	+45°	
9	M21EV/IMA	0°	
10	M21EV/IMA	-45°	
11	M21EV/IMA	-45°	
12	M21EV/IMA	0°	
13	M21EV/IMA	+45°	
14	M21EV/IMA	0°	
15	M21EV/IMA	90°	
16	M21EV/IMA	0°	
17	M21EV/IMA	-45°	
18	M21EV/IMA	0°	
19	M21EV/IMA	+45°	
20	M21EV/IMA	0°	

Nbr. Of plies	Orientation
10	0°
2	90°
4	+45°
4	-45°

Figure 1. The stacking sequence inside the composite plates.

The test samples were intended to besubjected in novel and conventional Non-Destructive Testing as well as mechanical testing (single lap shear joints). For this purpose, the test samples were fabricated based on a variation of the ISO 4587 standard, as illustrated in figure 2 (the dimensions refer to mm). For each NDT method two (2) test sample were used as Reference and four (4) as “Defected” samples.

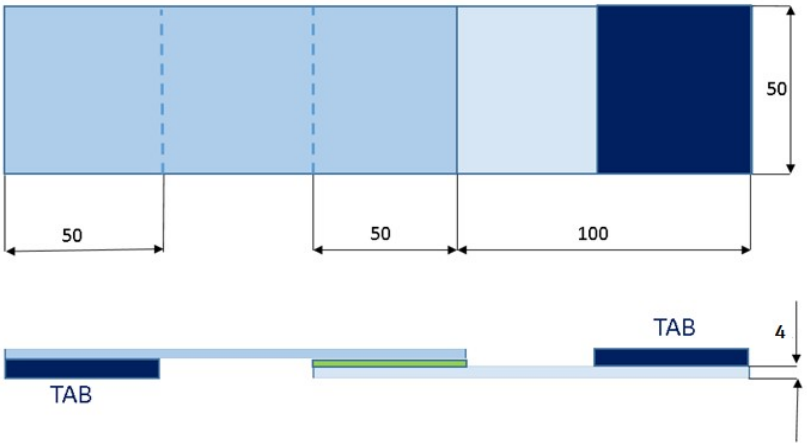

Figure 2. The geometry and dimensions of the test sample

3.2 Bonded joint preparation method (GMI Aero)

Smaller panels were cut out from the original composite panels according to the desirable dimensions. The cutting could be done using a table saw equipped with a diamond disk. The overlap area was marked by masking tape and abraded using sandpaper of 180 grit. For the Reference samples both sides were abraded while on “Defected” samples only one side is abraded. After the sanding, the overlap was cleaned thoroughly using Diestone cleaner.

The “Defected” samples were fabricated by contaminatingthe non-abraded overlap area. In this study, Lithium Grease (WD40 or similar) is applied on the surface, as illustrated in figure 3. Using a spatula it is possible to create a uniform thin layer of grease. Before bonding, the grease was left to dry for 24 hours.

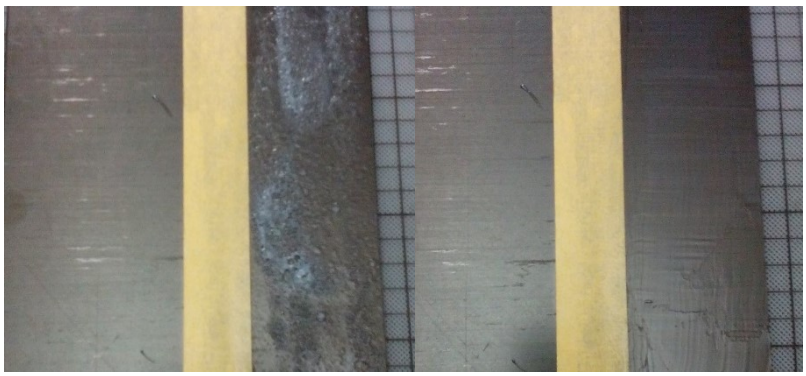

Figure 3. The Lithium Grease is applied on the non-abraded overlap area using a spatula.

The composite platesare bonded together using an adhesive film and by applying pressure and heat. This process could be performed in an autoclave ovenor by using the hot bonder ANITA(GMI AERO) and a heating blanket. In this example the bonding is done using aeronautical grade adhesive film FM 300M.The cure cycle as stated in the data sheet is 177 ^{o}C for 60 min. It is recommended to use an aluminum tape in order to secure the plates during the bonding process and also to prevent the adhesive from leaking. The bonding process is described below and illustrated in figure 4:

Figure 4. Out of autoclave curing using the hot bonder ANITA (GMI AERO) and a heating blanket

- Thermocouples provide temperature measurements for monitoring and control of the curing process.
- Strips of the same thickness (the alignment tabs for example) are placed underneath the plates and also close to the overlap area acting as supports.
- The heating blanket is placed above the composite plates and negative pressure is applied using a vacuum bag and a vacuum pump (in this example pressure = -0.8 bar).
- The cure cycle is set to 180 ^{o}C for 70 min (3^{o}C/min rise) in order to ensure the complete polymerization of adhesive.

After the completion of the curing process the aluminum tape was removed and the composite plates were cleaned with Acetone. Before bonding the alignment tabs (of the same composite material), the surface is abraded with sandpaper of 180 grit. The tabs are bonded using epoxy or acrylic adhesive by applying pressure with clamps in room temperature.In the final stage orthogonal stripswere cut out from the bonded plates in order to form the test samples. A portion of each side of the plates should be discarded (approximately 20 mm). In a second step the edges of the test samples were sanded using dry sand paper of 300 grit. Thecomplete set of test samples is presented in figure 5.

Figure 5. The complete set of test samples for each NDT method

4. NDT techniques for kissing bond defect detection

In this work, NDT techniques are used to investigate the test samples for the detection of kissing bond defects. NDT techniques namely (i) Guided wave NDT (ii) Laser shock (iii) High frequency C-scan (iv) Computed tomography are chosen for experimental investigation.Technical details of the testing techniques and experimental setup are given below.

4.1 Guided wave NDT

A detailed procedure following which the test samples panels and bonded joints are created is presented in Section 3.A picture of the test samples after the bonded joint is created is shown in Fig. 5. For the purpose of guided waves NDT inspection of the bonded joints, a different geometry is created keeping the bonded joint dimensions the same. This is to facilitate enough space for the guided waves to be created. The dimensions of tests samples for guided wave NDT inspection are presented in Fig 6(a). Fig 6(b) and 6(c) show the actual test samples with transducers attached. The transducers are attached in such a way that the guided waves pass through the entire length of the test sample including bonded joint before measurement. A total of six test samples are used for guided wave NDT inspection. There are two test samples without kissing bond defects and four test samples with kissing bond defects.

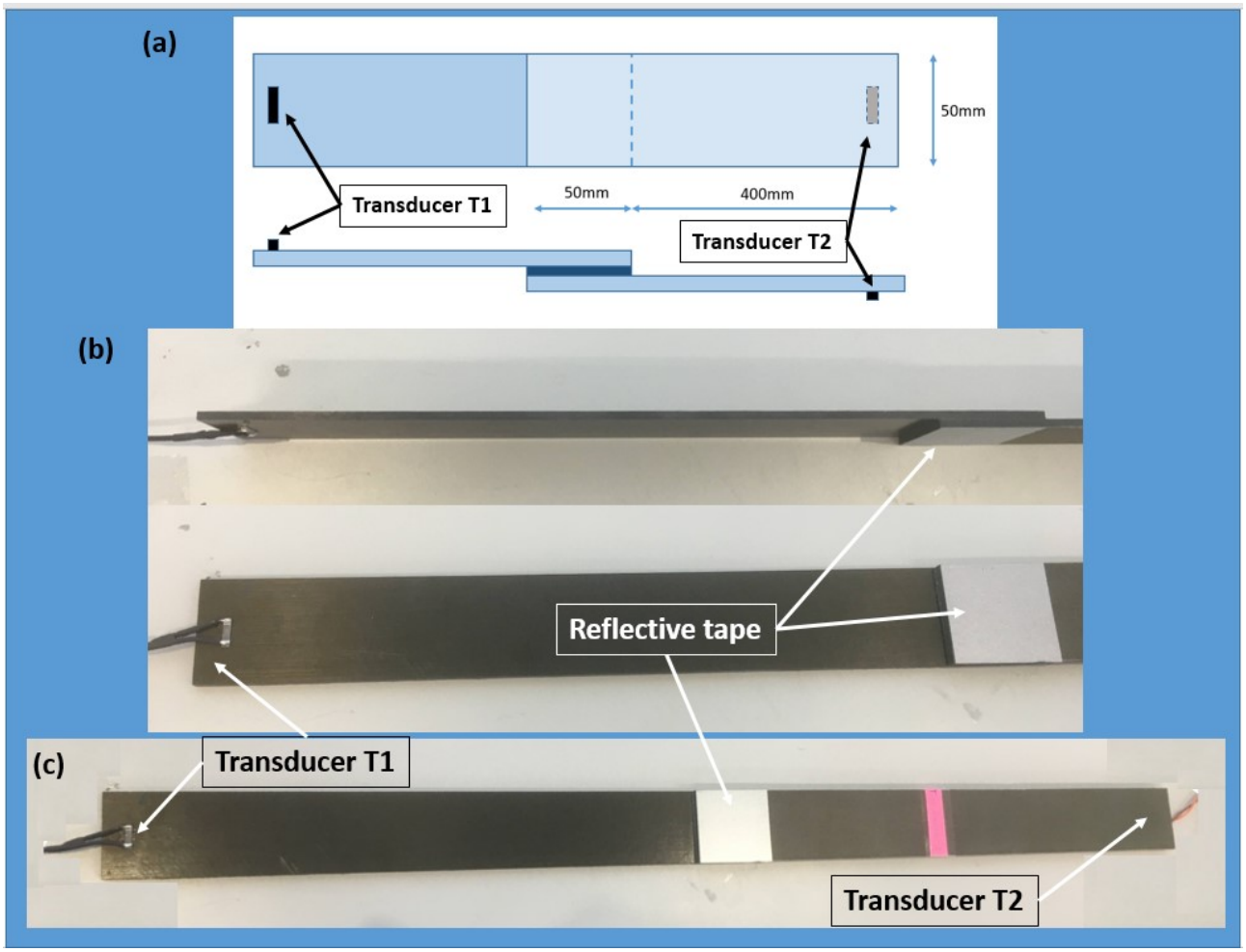

Figure 6: Test sample geometry for guided wave NDT

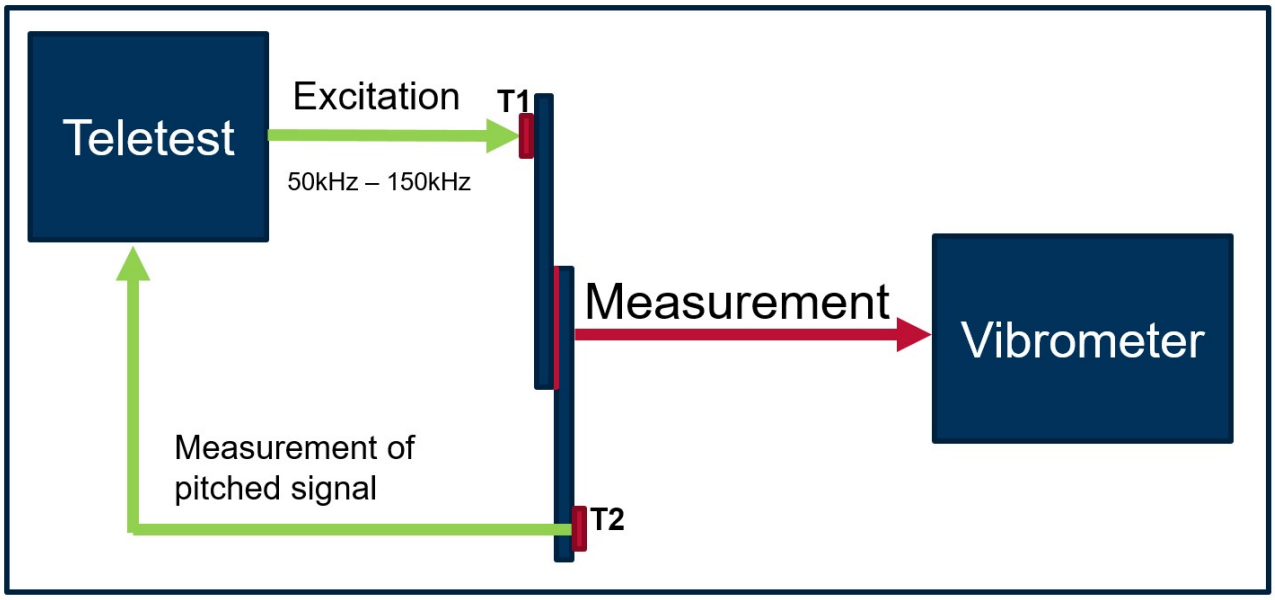

Figure 7: Test samples of guided wave NDT

The test samples are attached with "ASS-3000-0070-B Fuzz Button Piezo Element & Bonded Face Plate" transducers from Eddyfy Technologies (see Fig 7). The transducers are made of piezo electric material, which vibrate at a wide range of frequencies. In order to excite the transducers with appropriate frequency, TELETEST Mk3 is used. The equipment is capable of generating frequencies up to 200kHz in various modes. It is capable of generating single, multiple and sweeping frequencies within certain lower and upper limit. It also offers various window for modulation. A laser-vibrometer from Polytech is used to measure the test sample surface velocity behavior while the guided waves are setup in the sample. The equipment is able to measure a frequency up to a max of 2MHz.

A block diagram of the experimental setup is presented in Fig 7. The experiments are conducted in two different configurations. In one configuration, TELETEST is used in pulse-echo mode. In another configuration, TELETEST is used to excite the transducer and the test sample response is read by a laser-vibrometer. Both the configurations are shown in the same block diagram in Fig 7. The experiments procedure of both configurations is discussed in the next sub-sections.

4.1.1. Measurements using TELETEST:

Measurements are carried out in pitch-catch mode. Transducers are attached to the test sample to facilitate the same (see Fig 7). Transducer 1 (T1) is used as input and Transducer 2 (T2) is used to read the test sample response to guided waves. T1 is excited with a sinusoidal signal of varying frequency from 50kHz to 150kHz sampled at of 1µs of chirp duration of 500µs with Tukey factor of 0.25. This excitation signal sets up guided waves in the test sample. The test sample behaviour to the guided waves is captured using T2 and is read by the TELETEST equipment. This test is repeated on all six test samples.

The recorded signals are presented in Fig 8. Figure 8(a) shows the amplitude-time plot of the received signal in all the test samples. Figure 8(a) shows the power spectral plot of the time signals shown in Fig 8(b). Plots with the title "REF Sample #" represent the response of the test sample without kissing bond defect and the plot with the title "Sample #" represent the response of the tests sample with kissing bond defect.Power spectral plots are presented in the amplitude-frequency domain with boxes for better interpretation of the results.

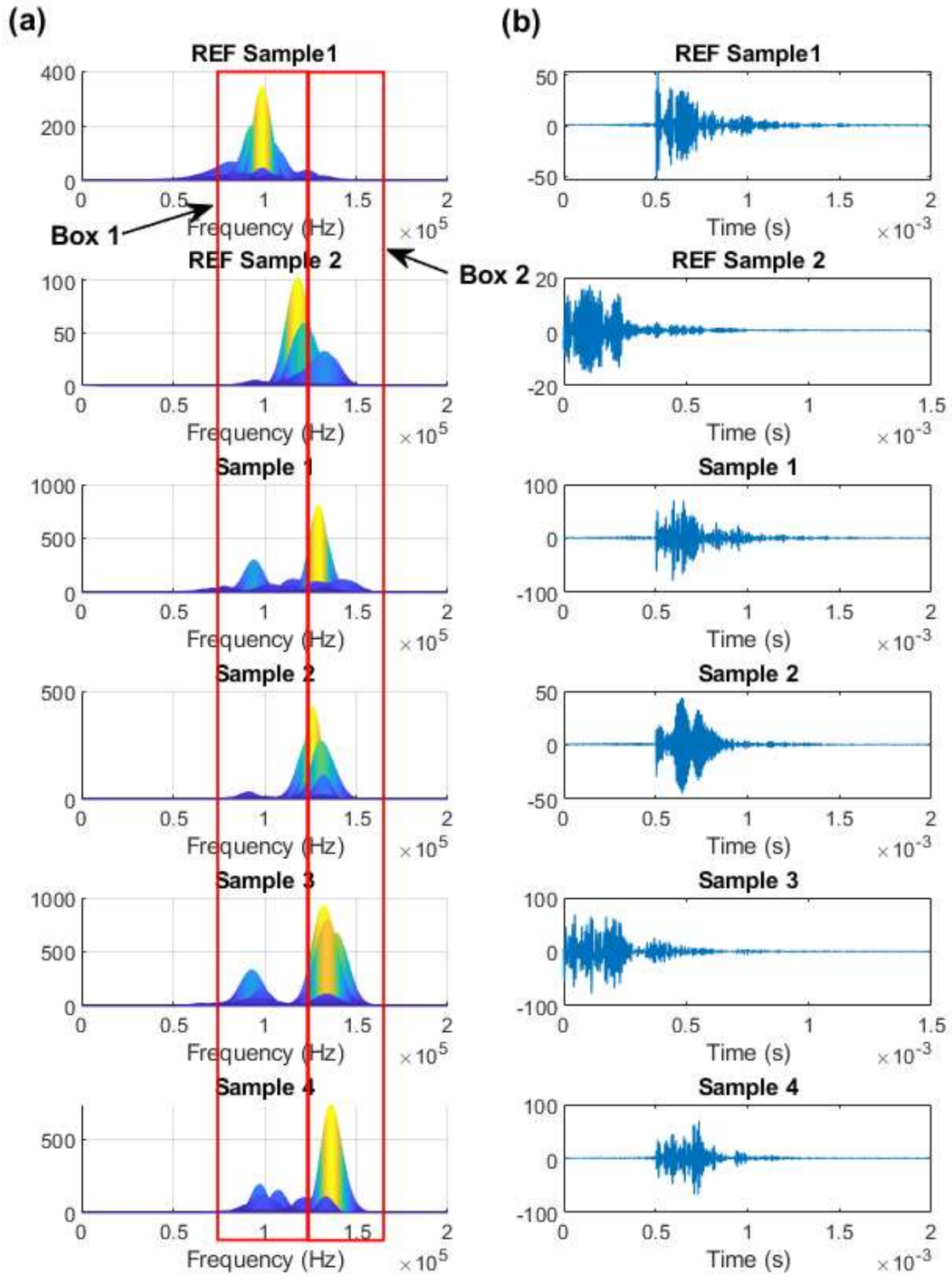

Figure 8:(a) Spectral plot of the time response in frequency domain (b) Time response of the test samples

It can be noted that the response of the "REF Samples" shows the highest amplitude occur at a frequency lower than 125 KHz. All major frequencies of high amplitude are present in the response of these samples are inside the "Box 1". Hence, the bonded joint in this case behaves like a low pass filter.

In all the plots with the name"Sample #"it shows that the highest amplitudes occur at a frequency higher than 125kHz. In this case,all the frequencies of high amplitude are in the "Box 2". This indicates that the bonded joint with kissing bond defect behaves like a high pass filter. There is a clear difference in the response of the samples with which kissing bond defects can be identified on the bonded joints.

4.1.2 Measurements using laser-vibrometer

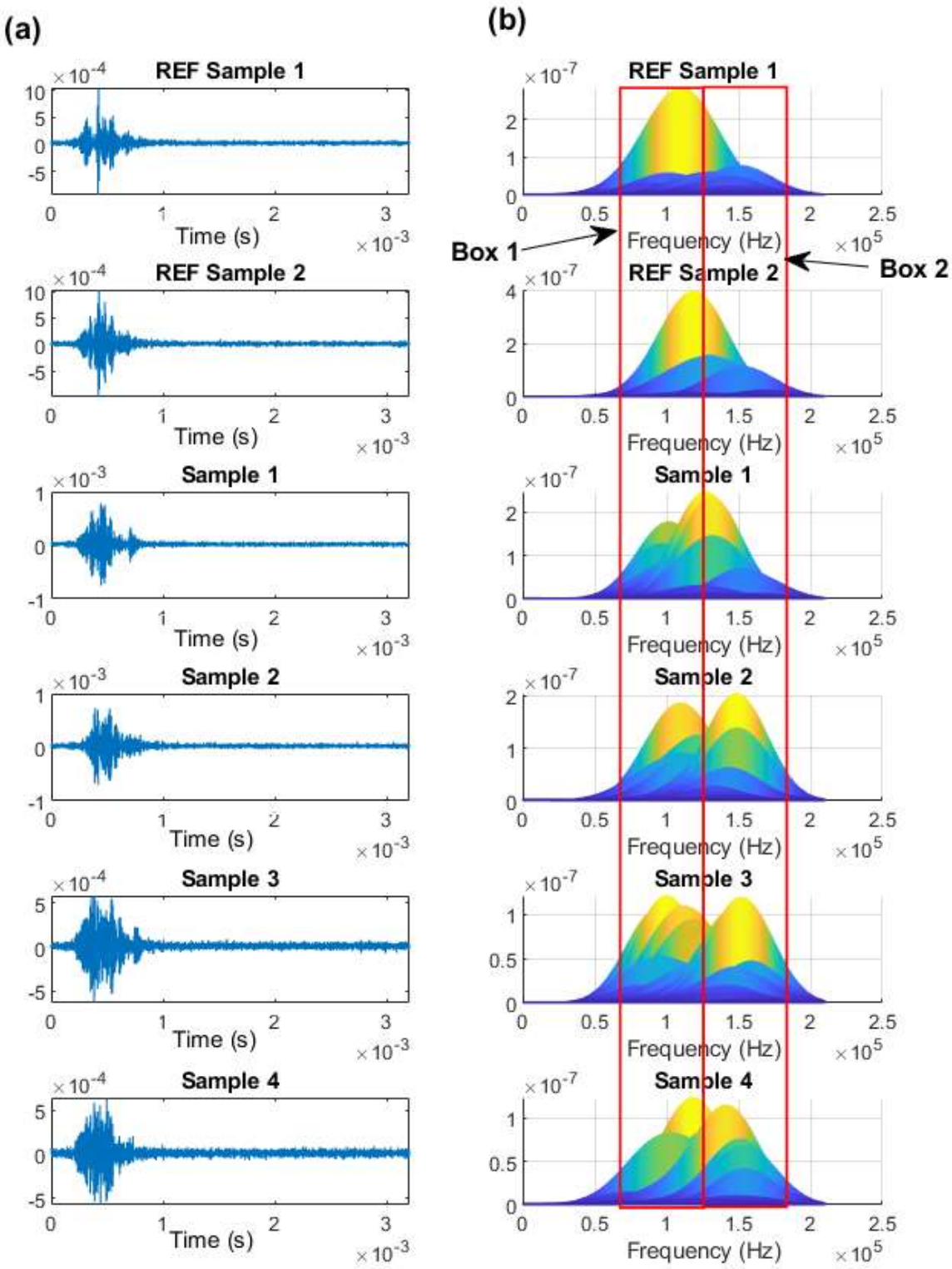

Figure 9: (a) Time signal measured at bonded joint (b) Spectrum plot of the time signal measured at bonded joint

In addition to the TELETEST experimental test setup mentioned in Section 4.1.1, laser-vibrometer of 2MHz capacity is used to measure the test sample behaviour while the guided waves are setup. The laser-vibrometer is focussed at a point on the bonded joint as shown in Fig 7. In this way the guided waves pass though the bonded joint before measurements are taken by the laser-vibrometer.

Excitation signal given to T1 is same as it is used in the case of TELETEST experiments (mentioned in Section 4.1.1). Measurements obtained using the laser-vibrometer are presented in Fig. 9. In the plots, Fig 9(a) shows the time signals of the guided waves measured at the bonded joint surface and Fig 9(b) represents the spectrum plot of the time signal on frequency domain. Two boxes are placed on the frequency domain

plots in Fig 9(b) for better interpretation of results. It can be noted from the plots that the frequencies of highest peaks are within the Box 1 for the test samples with no kissing bond defects. In the case of the test samples with kissing bond defects, the frequencies of the highest peaks are within the Box 2. There exists some frequencies in both the boxes in the case of test samples with kissing bond defects. This can be attributed to the noise induced due to the non-invasive measurements made using the laser-vibrometer.

4.2Laser shock test

It is well known from the literature thata material when subjected to a laser shock, develops plasma on the material surface due to high energy impact within a small area. The plasma creates a shock pulse within the material. The shock pulse creates tensile and stresses in the material while it reflects back and forth between the material surfaces.The test sample surface starts vibrating while the shock pulse is setup within the material. This can be captured to study the material behaviour.

As long as the energy input by the shock pulse does not create a tensile strength higher than the yield strength of the material, the test is non-destructive. This can be primarily confirmed by examining the test sample surface where it is subjected to the laser shock.

A pulsed Nd:Yag laser of 1064nm, 2.7J energy, 10ns pulse is used in these tests. Laser is used to shock the test sample and a laser-vibrometer (of 24MHz) from Polytech is used to measure the back surface velocity of the test sample when it is chocked with the laser pulse. Schematic of the test setup is presented in Fig 10.
The test setup is created using a rigid frame fixed to a rigid base. The test samples are held tight on the rigid frame. The rigid frame setup is positioned in between the pulsed laser and the laser-vibrometer.

There are two samples without kissing bond defect and six samples with kissing bond defects which total to 8 samples for laser shock tests.For laser shock experiments, the test sample dimensions are as shown in Fig 2. Test sample is prepared for the laser shock tests in order to make sure no damage to material of the samples. A sacrificial layer (a black tape) is placed on the bonded joint of the test sample. A reflective tape is placed in the opposite side of the bonded joint to ease the laser-vibrometer measurements. The sample with sacrificial layer is fixed on the rigid frame so that sacrificial layer side of the sample faces pulsed laser.A thin layer of continuous water flow is maintained over the sacrificial layer during the laser shock. The water layer confines all the laser energy over the surface of the test sample.Laser-vibrometer is focussed on the reflective side of the test sample. It is made sure that the laser-vibrometer picks up the test sample velocity at the same point on the reflective side of the test sample where it is subjected to laser shock pulse in the opposite side.

Laser shock tests are conducted with 2.16J, 1064nm and 10ns. Laser-vibrometer is configured to measure velocity at each nano second resolution. The test sample is subjected to one laser shock and back surface velocity is recorded by laser-vibrometer. Velocity measurement is carried out until the back surface velocity reads to the pre-shock condition. Each sample is subjected to five laser shocks with five minute time interval in order to obtain the best results. The tests are repeated five times on each sample because there is no provision to obtain averaged signal. Sample must be subjected to several laser shocks at a time in order to obtained the averaged back surface velocity. Subjecting the samples to several laser shocks damages the test samples. The time interval between the five tests on a single sample is to make sure the test sample is in place and dissipate heat. After each laser shock, the water flow is stopped, the test sample is repositioned so that the next laser shock will be at another location and then the water flow is switched on for the next test.

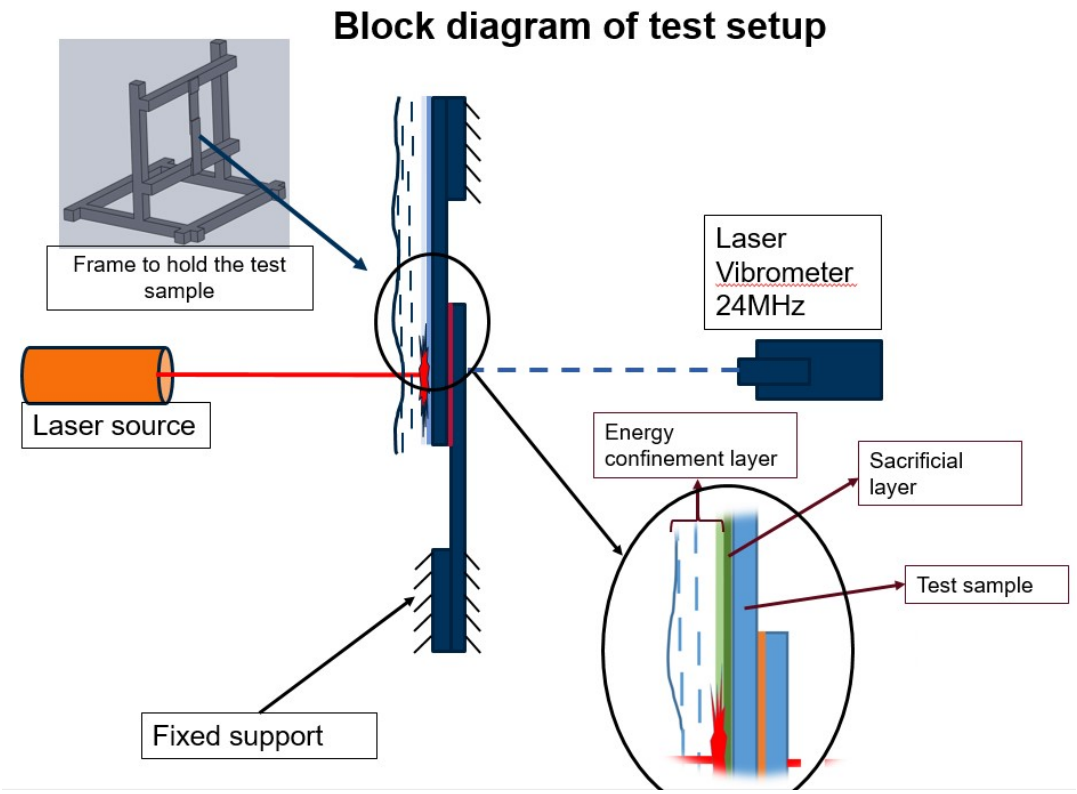

Figure 10: Block diagram of laser shock test setup

Measurements are carried out on all the samples. The label “Ref sample #” represents the test sample with out kissing bond defect and the label “sample #” represents the test sample with kissing bond defect. The best result from the five tests on each sample is presented in Fig 11. Figure 11(a) shows the back surface velocity of the test sample in time domain. A spectral plot of the time signals in frequency domain is presented in Fig 11(b).

Laser shock tests closely simulate impulse excitation test of mechanical systems. The laser shock approximates an impulse because all energy of the laser is dissipated to the test sample within few nano-seconds. The response of the test sample to such an input excitation contains the system characteristics. Hence, the plots presented in Fig 11 are the impulse responses of the test samples in both time and frequency domain. As the impulse response contains the system characteristics, plots in Fig 11 represent the characteristics of both material, bonded joint and defect information. It can be better visualised in frequency domain (Fig 11(b)) than in the time domain (Fig 11(a)).

To illustrate the difference in the response of samples with kissing bond defect and without kissing bond defect a two window box is placed on the plots at 250kHz. It can be observed that the frequencies with higher amplitudes are within Box1 in the case of test samples without kissing bond defect. The frequencies with higher amplitude in the case of test samples with kissing bond defect are within Box2. The plots clearly distinguish the difference between test samples with kissing bond defect and the test samples without kissing bond defect. However, “Sample 1” shows a similar trend to “EEF Sample 1 &2”.

In the case of laser shock tests also, the analogy of high-pass, low-pass filter is valid as the response of the test samples with kissing bond defect against laser shock is on the higher frequency in comparison with the response of the test samples without kissing bond defect.

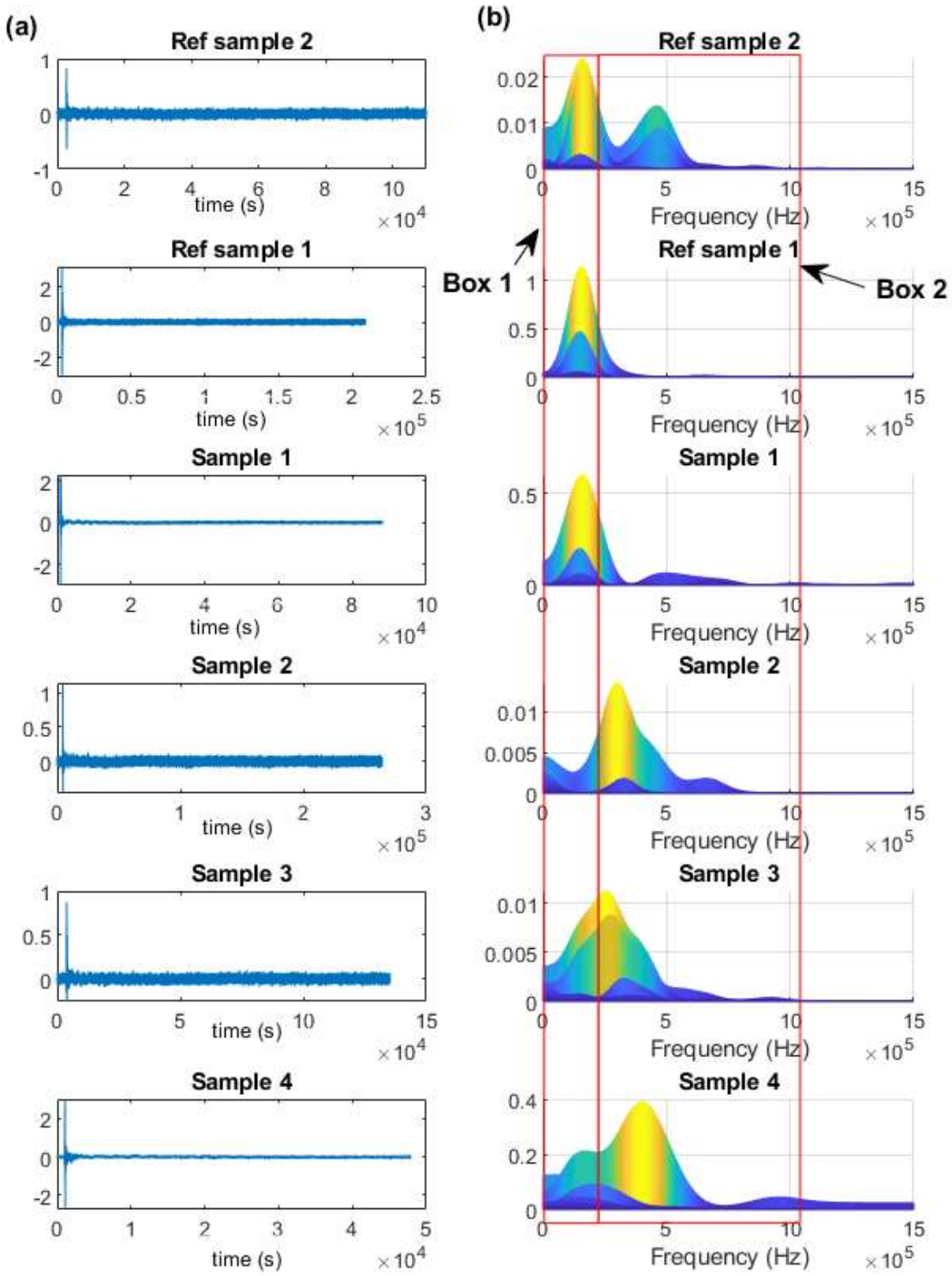

Figure 11: (a) Back surface velocity in time domain (b) Back surface velocity spectral plot on frequency domain

4.3 High frequency C-scan

Similar to guided wave mentioned earlier in the document, High-frequency C-scanning utilises high frequency sound within the ultrasound range to non-destructively test the sample. For SWAK, high-frequency probes of frequencies 5MHz, 10MHz and 15MHz were used in an immersion set up. Immersion testing involves immersing the sample within a medium, in this case water, and positioning the probe at a set offset before scanning over with a 0° probe (See Figure 12). The probe used acts as both a transducer and receiver in a pulse-echo practice.

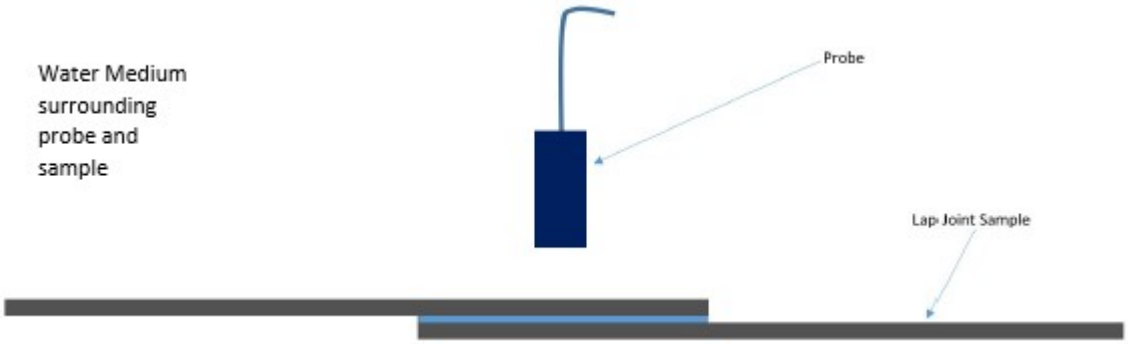

Figure 12: Immersion Tank Set Up

Once the reflected sound wave is received by the probe, an ultrasonic A-scan and C-scan can be created to present the data. The ultrasonic A-scan is a conventional NDT technique used to inspect materials and displays the reflected pulse amplitude (in dB) represented along the Y axis with time or distance presented along the X axis. The presented A-scan displays information at a particular point of interest within the material. Alongside this, an Ultrasonic C-scan can also be created to present information over a wide range or sample surface (See Figure 13). It is a two-dimensional scan of a specimen that maps parameters such as reflected wave amplitude as a function of the location over the samples surface. The C-scan gives a plan view of the samples, including any defects, and is often an automated process that is used to map out lamination like indications.

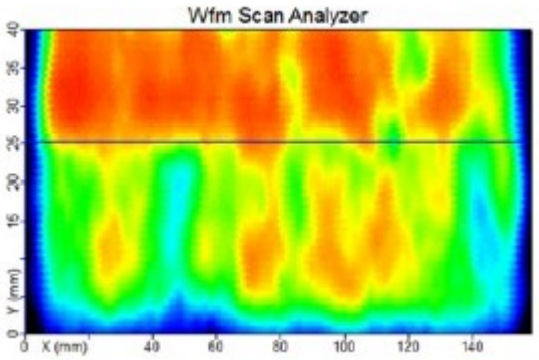

Figure 13: C-scan of Composite Reference Sample

As previously stated, each samples was inspected with a variety of probes ranging from 5MHz to 15MHz and were all set up as unfocussed scans. Scanning was carried out at 0.5mm XY resolution with the time-base scale set to the sound velocity of carbon fibre. The inspection software recorded the C-scan data, along with any associated A-scans, and saved with appropriate file names to ensure no identification errors. Generally, with UT testing an increase in frequency results in a decrease in wavelength. Hence, by increasing the frequency the sensitivity and attenuation of the scan increases. Attenuation can be classed as the energy lost through scatter and material absorption within the material. Therefore, although an increase in frequency results in an increased sensitivity, the internal fibres of the composite sample result in high attenuation and dramatically reduced the signal penetration. Generally a lower frequency is selected when inspecting composites as a compromise between penetration and sensitivity/resolution.

As KB defects are classed as a zero-volume defect, generally a lower frequency probe does not provide the sensitivity and resolution required to detect it. Therefore a higher frequency was selected for SWAK.

Initial inspections were carried out on the 6 samples created, 2 reference samples and 4 contaminated samples, with results proving difficult to interpret. As expected, the internal fibres of the samples resulted in a noisy response with geometrical features difficult to identify. Scans were conducted on each side of the sample, as the location of the contamination layer is unknown, with each sample being labelled with an A and B side.

To aid with data analysis, flat bottom holes (FBH) were drilled into a previously used section of composite sample at depths of 1mm, 2mm and 3mm. Immersion testing of these samples is scheduled to be conducted in August 2021 with inspections focussing on areas above the back wall and each FBH (see Figure 14). The three different samples contained the various features:

- Sample 1: 3 x 2mmØ FBH
- Sample 2: 3 x 3mmØ FBH
- Sample 3: 3 x 4mmØ FBH

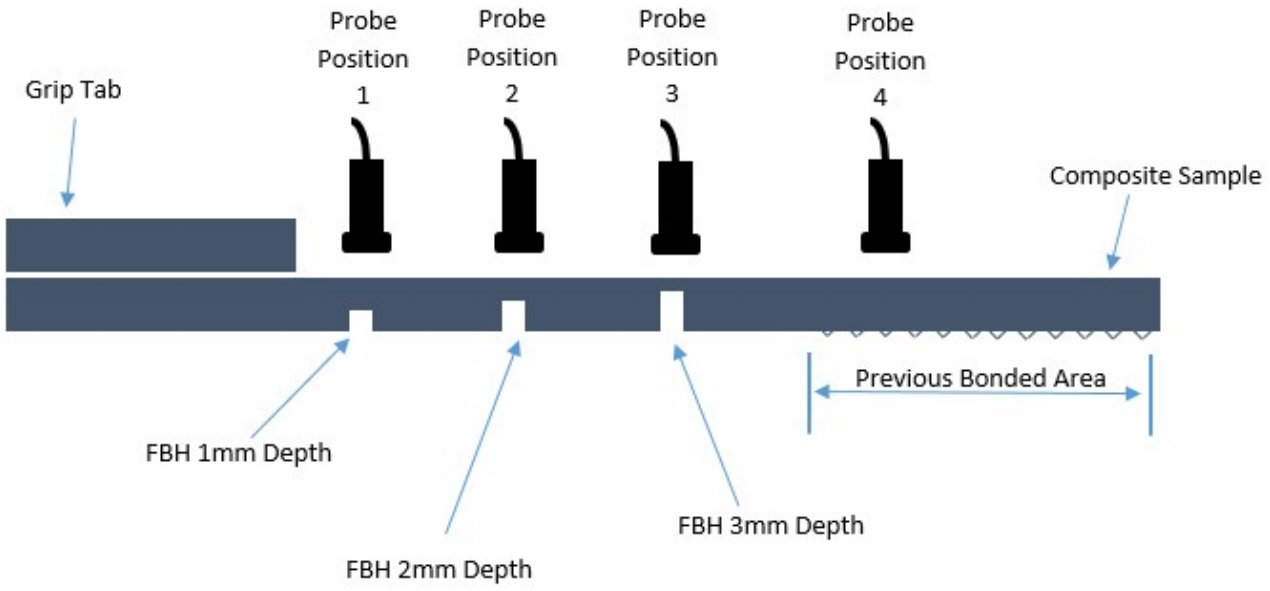

Figure 14: Additional Testing Sample to Aid in Composite Sample Data Analysis

4.4 Computed tomography

The set of test samples contained two reference samples and four contaminated samples. As with the other specimens, it is unknown which surface of the adherends had the contamination layer applied and so both sides A and B of the joints needed to be tested and investigated (see Figure 15).

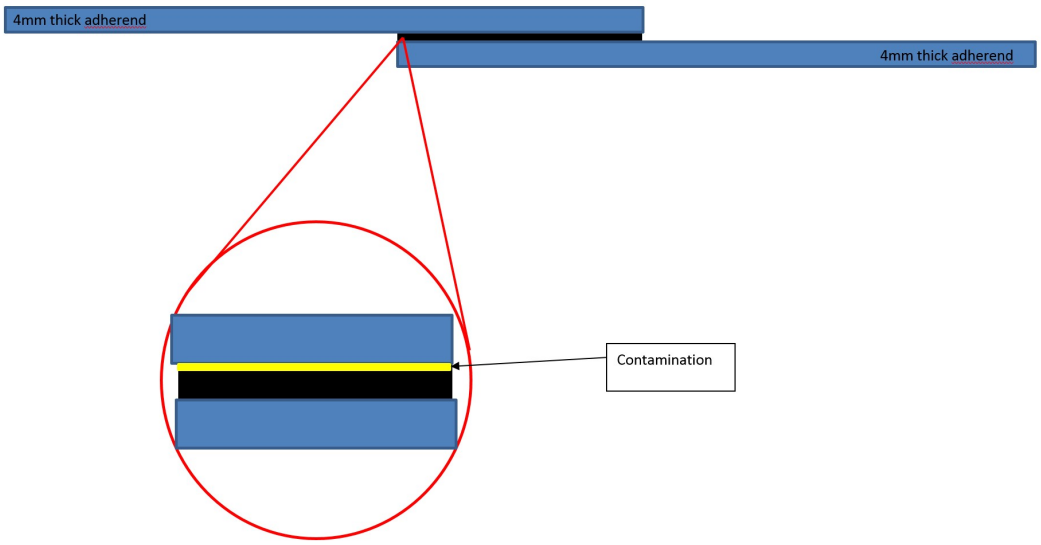

Figure 15: Schematic of Contamination Layer in SWAK Composite Lap Joint [1]

XCT is a radiographic based imaging NDT method that produces 2D cross-sectional images alongside 3D volumetric images. The images can then be analysed to identify internal structures, dimensions, defects and density. The set up for XCT involves an X-ray source located on one side of the sample under test with an X-ray detector located on the opposite side (see Figure 16). The X-ray source then generates an X-ray beam that propagates through the test sample before being detected by the X-ray detector. The detector can identify variations in the beam intensity created by internal features of the samples. The test is repeated, at various angles in relation to the test specimen to create a stacked 2D image. The 2D images can then be further processed with added grey-scale values added to create a 3D image directly related to the test materials density and geometrical properties.

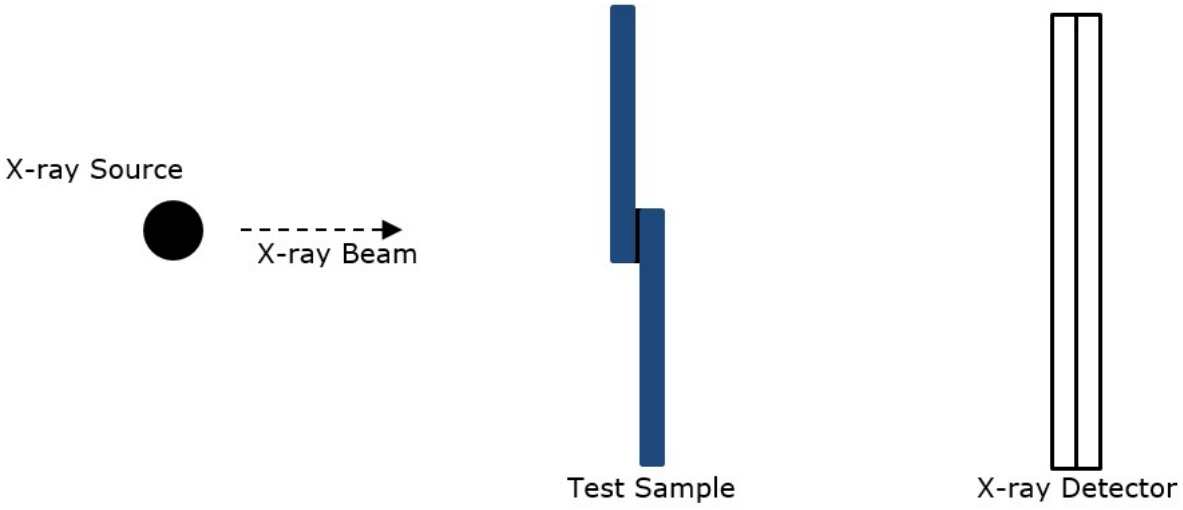

Figure 16: Schematic of XCT Set Up

Analysis of the generated 3D images involves reviewing the data into three orthogonal CT slice views of Top, Right and Front (See Figure 17). These orthogonal views allow analysis for the full cross section of each sample.

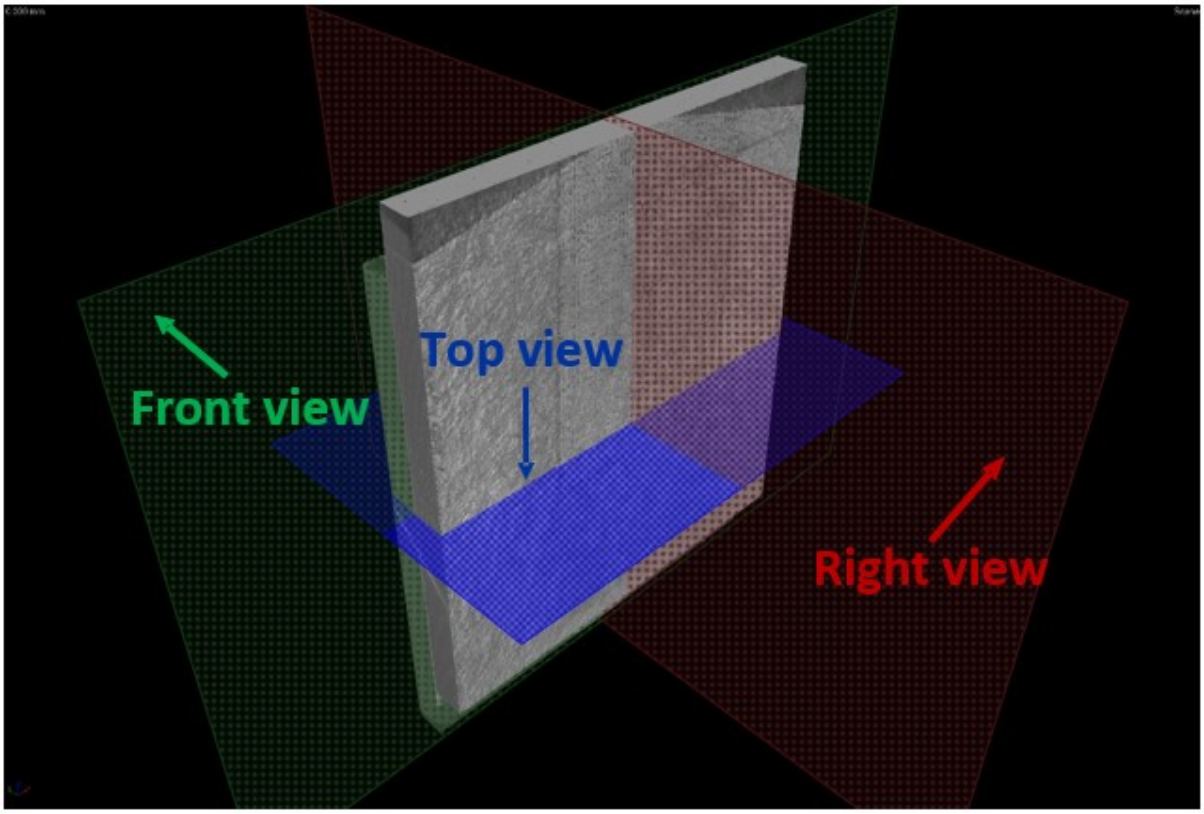

Figure 17: Orthogonal Views of 3D XCT Image [1]

Examples of the XCT orthogonal views from one of the SWAK composite lap joint samples can be seen in Figures 18 to 20. Further analysis of the XCT data will be detailed in TWI Report 32989_1v1_21 *XCT of six composite single lap joint samples*.

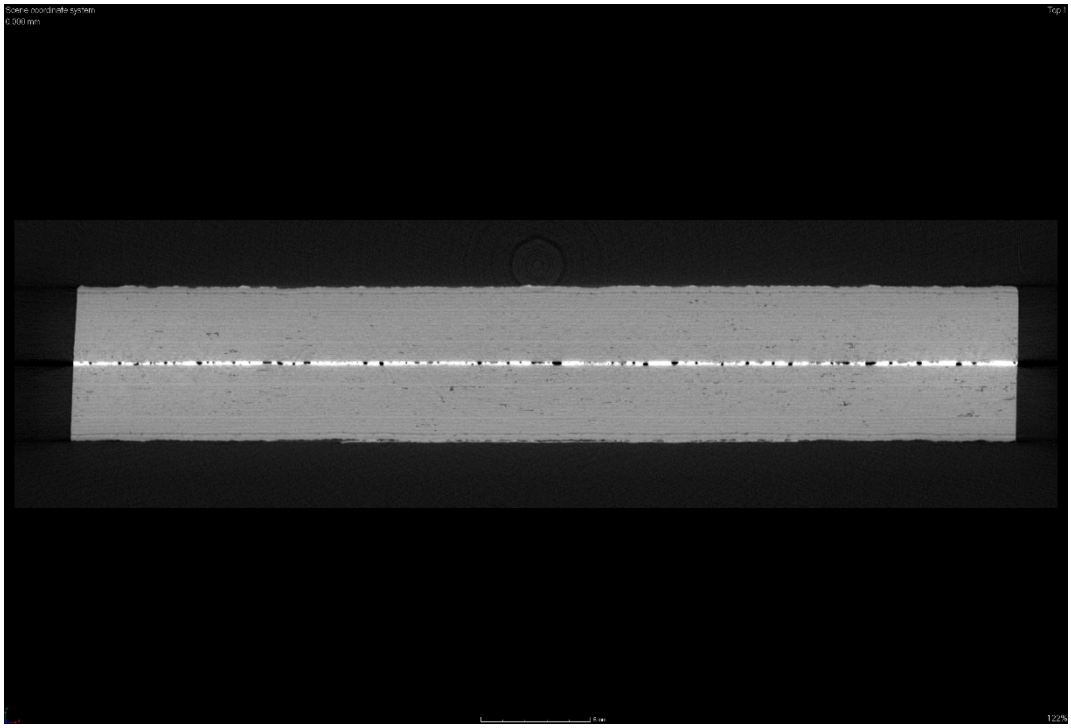

Figure 18: Top View CT Slice Image

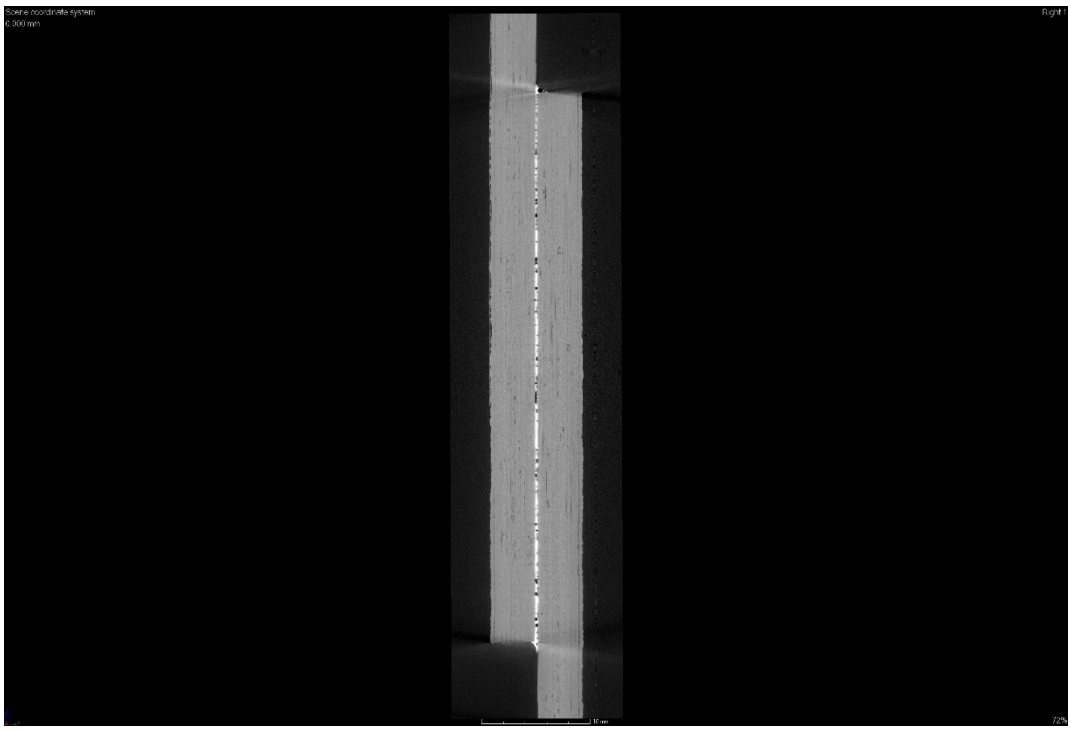

Figure 19: Right View CT Slice Image

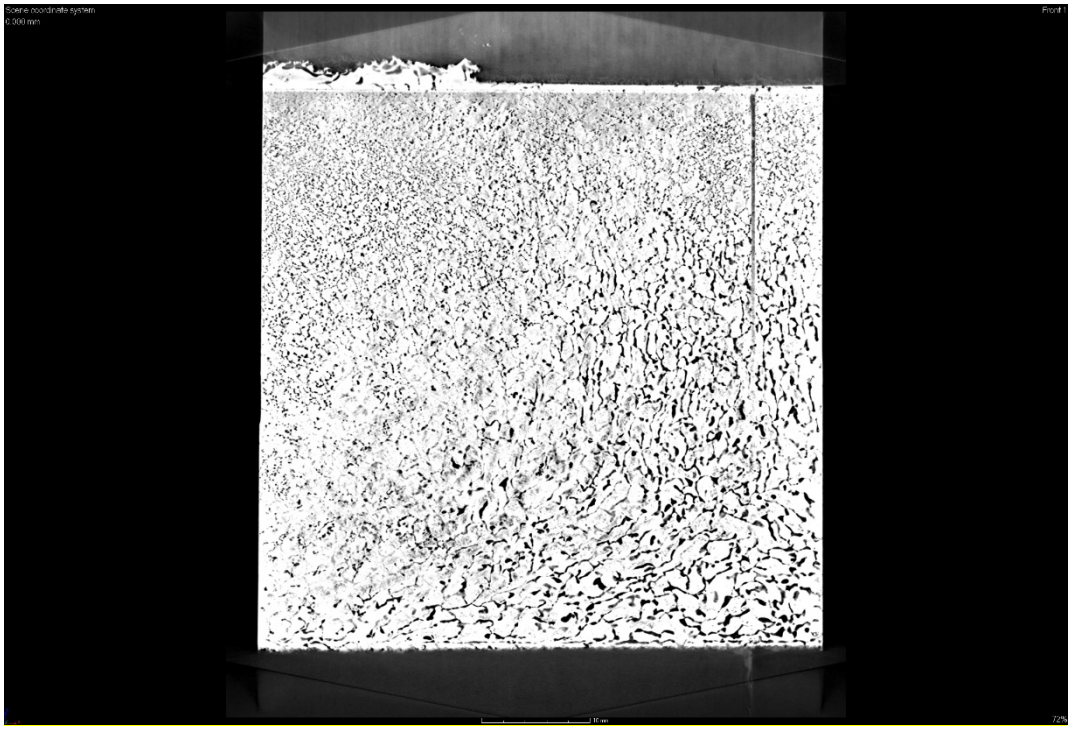

Figure20: Front View CT Slice Image

5. Conclusions

The aim of this work is to evaluate advanced NDT methods to identify bonded joints with kissing bond defects.For this purpose, a technique is developed to create composite bonded joints with kissing bond defects. A protocol is formulated upon validating the bonded joints with mechanical destructive testing. Another set of test samples are fabricated to evaluate advanced NDT methods. The methods are (1) Guided

waves NDT (2) Laser shock (3) High frequency C-scan (4) Computed tomography. Time-frequency analysis is used to analyse the test results of Guided wave NDT and Laser shock tests. The results of both the methods show that the methods are effective in identifying the bonded joints with kissing bond defect. However, there is some degree of failure to identify bonded joints with kissing bond defects. The other two techniques are close to completion for the final assessment.

6. References

[1]. Wood, Michael, Peter Charlton, and Dawei Yan. "Ultrasonic evaluation of artificial kissing bonds in CFRP composites." The e-Journal of NDT 19.12 (2014).

[2]. Droździel, Magda, et al. "The mechanical effects of kissing bonding defects in hybrid metal-composite laminates." Composite Structures 269 (2021): 114027.

[3]. Marty, Pierre Noël, N. Desai, and J. Andersson. "NDT of kissing bond in aeronautical structures." 16th world conference on NDT. 2004.

[4]. Chen, Bo-Yang, et al. "A vibro-acoustic modulation method for the detection of delamination and kissing bond in composites." Journal of Composite Materials 50.22 (2016): 3089-3104.

[5]. De Luca, A., et al. "Damage characterization of composite plates under low velocity impact using ultrasonic guided waves." Composites Part B: Engineering 138 (2018): 168-180.

[6]. Zou, Fangxin, Jing Rao, and M. H. Aliabadi. "Highly accurate online characterisation of cracks in plate-like structures." NDT & E International 94 (2018): 1-12.

[7]. Wan, Xiang, et al. "Numerical study on static component generation from the primary Lamb waves propagating in a plate with nonlinearity." Smart Materials and Structures 27.4 (2018): 045006.

[8]. Loveday, Philip W., Craig S. Long, and Dineo A. Ramatlo. "Mode repulsion of ultrasonic guided waves in rails." Ultrasonics 84 (2018): 341-349.

[9]. Heinlein, Sebastian, et al. "Blind trial validation of a guided wave structural health monitoring system for pipework." Materials Evaluation 76.8 (2018): 1118-1126.

[10]. Lowe, M. J. S., G. Neau, and M. Deschamps. "Properties of guided waves in composite plates, and implications for NDE." AIP Conference Proceedings. Vol. 700. No. 1. AIP, 2004.

[11]. Rokhlin, S. I. "Lamb wave interaction with lap-shear adhesive joints: Theory and experiment." The Journal of the Acoustical society of America 89.6 (1991): 2758-2765.

[12]. Singher, Liviu. "Bond strength measurement by ultrasonic guided waves." Ultrasonics 35.4 (1997): 305-315.

[13]. Duflo, H., B. Morvan, and J-L. Izbicki. "Interaction of Lamb waves on bonded composite plates with defects." Composite structures 79.2 (2007): 229-233.

[14]. Teles, Sorin V., and D. E. Chimenti. "Closed disbond detection in marine glass-epoxy/balsa composites." NDT & E International 41.2 (2008): 129-136.

[15]. Ren, Baiyang, and Cliff J. Lissenden. "Ultrasonic guided wave inspection of adhesive bonds between composite laminates." International Journal of Adhesion and Adhesives 45 (2013): 59-68.

[16]. Koodalil, Dileep, et al. "Detection of interfacial weakness in a lap-shear joint using shear horizontal guided waves." NDT & E International 112 (2020): 102248.

[17]. Balasubramaniam, Kaleeswaran, et al. "Ultrasonic Guided Wave Signal Based Nondestructive Testing of a Bonded Composite Structure Using Piezoelectric Transducers." Signals 2.1 (2021): 13-24.

[18]. Gao, Tianfang, et al. "Multi-frequency localized wave energy for delamination identification using laser ultrasonic guided wave." Ultrasonics 116 (2021): 106486.

[19]. Carcione, A., et al. "Modulated high frequency excitation approach to nonlinear ultrasonic NDT." *Journal of Sound and Vibration* 446 (2019): 238-248.

[20]. Łopato, Przemysław, Tomasz Chady, and Ryszard Sikora. "Testing of composite materials using advanced NDT methods." *COMPEL-The international journal for computation and mathematics in electrical and electronic engineering* (2011).

[21]. Łopato, Przemysław, Tomasz Chady, and Ryszard Sikora. "Testing of composite materials using advanced NDT methods." *COMPEL-The international journal for computation and mathematics in electrical and electronic engineering* (2011).

[22]. Yılmaz, Bengisu, and Elena Jasiūnienė. "Advanced ultrasonic NDT for weak bond detection in composite-adhesive bonded structures." *International Journal of Adhesion and Adhesives* 102 (2020): 102675.

[23]. Yılmaz, Bengisu, and Elena Jasiūnienė. "Advanced ultrasonic NDT for weak bond detection in composite-adhesive bonded structures." *International Journal of Adhesion and Adhesives* 102 (2020): 102675……..

[24]. Blouin, Alain, et al. "Applications of Laser-Ultrasonics and Laser Tapping to Aerospace Composite Structures." (2008): 1-7.

[25]. Gupta, V., et al. "Measurement of interface strength by laser-pulse-induced spallation." *Materials Science and Engineering: A* 126.1-2 (1990): 105-117.

[26]. Yuan, J., and V. Gupta. "Measurement of interface strength by the modified laser spallation technique. I. Experiment and simulation of the spallation process." *Journal of Applied Physics* 74.4 (1993): 2388-2396.

[27]. Gupta, V., and J. Yuan. "Measurement of interface strength by the modified laser spallation technique. II. Applications to metal/ceramic interfaces." *Journal of Applied Physics* 74.4 (1993): 2397-2404.

[28]. Yuan, J., and V. Gupta. "Measurement of interface strength by the modified laser spallation technique. I. Experiment and simulation of the spallation process." *Journal of Applied Physics* 74.4 (1993): 2388-2396.

[29]. Gupta, V., and J. Yuan. "Measurement of interface strength by the modified laser spallation technique. II. Applications to metal/ceramic interfaces." *Journal of Applied Physics* 74.4 (1993): 2397-2404.

[30]. Yuan, J., V. Gupta, and A. Pronin. "Measurement of interface strength by the modified laser spallation technique. III. Experimental optimization of the stress pulse." *Journal of Applied Physics*74.4 (1993): 2405-2410.

[31]. Asay, James R., and Mohsen Shahinpoor, eds. *High-pressure shock compression of solids*. Springer Science & Business Media, 2012.

[32]. Blouin, Alain, et al. "Applications of Laser-Ultrasonics and Laser Tapping to Aerospace Composite Structures." (2008): 1-7.

[33]. Perton, Mathieu, Alain Blouin, and Jean-Pierre Monchalin. "Adhesive bond testing of carbon–epoxy composites by laser shockwave." Journal of Physics D: Applied Physics 44.3 (2010): 034012.

[34]. Ecault, Romain, et al. "A study of composite material damage induced by laser shock waves." Composites Part A: Applied Science and Manufacturing 53 (2013): 54-64.

[35]. Gay, Elise, et al. "Study of the response of CFRP composite laminates to a laser-induced shock." *Composites Part B: Engineering* 64 (2014): 108-115.

[36]. Ehrhart, Bastien, et al. "Development of a laser shock adhesion test for the assessment of weak adhesive bonded CFRP structures." International Journal of Adhesion and Adhesives 52 (2014): 57-65.

[37]. Ghrib, Meriem, et al. "Generation of controlled delamination in composites using symmetrical laser shock configuration." Composite Structures171 (2017): 286-297

[38]. Sagnard, Maxime, et al. "Development of the symmetrical laser shock test for weak bond inspection." *Optics & Laser Technology* 111 (2019): 644-652.Sagnard, Maxime, et al. "Development of the symmetrical laser shock test for weak bond inspection." Optics & Laser Technology 111 (2019): 644-652.

[39]. Bossi, Richard H., Karen K. Cooprider, and Gary E. Georgeson. *X-ray computed tomography of composites*. Boeing Aerospace And Electronics Co Seattle Wa, 1990.

[40]. Green, William H., and Patrick Sincebaugh. *Nondestructive evaluation of complex composites using advanced computed tomography (CT) imaging*. ARMY RESEARCH LAB ABERDEEN PROVING GROUND MD, 2001.

[41]. A. Jansson, J. Ekengren, A.-R. Zekavat, L. Pejryd, Effects of X-ray penetration depth on multi material computed tomography measurements, in: 6th Conference on Industrial Computed Tomography, 2016, 8 pp.

[42]. M. Krumm, S. Kasperl, M. Franz, Reducing non-linear artifacts of multi-material objects in industrial 3D computed tomography, NDT E Int. 41 (4) (2008) 242–251.